

Mechanisms of Cracking in Pure Magnesium During High Strain Rate Plastic Deformation

Pawel Nowakowski*, Mary Ray, Paul Fischione

E.A. Fischione Instruments, Inc. Export, PA U.S.A.
Corresponding author: p_nowakowski@fischione.com

Understanding metal failure at high rates of deformation is a prevalent problem for many industrial applications, such as shock absorption, structural engineering, and formability processes. The failure of materials can be observed under dynamic loading, due to plastic instability caused by severe and dynamic microstructural transformation. This severe plastic deformation manifests through the formation of adiabatic shear bands (ASB) [1-4]. In alloys, the ASB is accompanied by dynamic recrystallization, which results in material softening that leads to crack formation [3, 5-8].

A sample of hot rolled pure magnesium (purity $\geq 99.5\%$) was rapidly deformed under dynamic two-directional bending conditions, in two cycles, two bands each. The deformation was carried out perpendicular to the rolling direction. Due to intrinsic characteristics of magnesium (easily damage during mechanical polishing), the sample was prepared using a broad argon ion beam (BIB) mill [Model 1062 TrionMill, Fischione Instruments]. An electron backscatter diffraction (EBSD) system [e-Flash^{FS}, Bruker Nano Analytics] was used on a focused ion beam (FIB) system [Scios, Thermo Fisher Scientific], which was operated at 15 kV for mapping the sample with a step size of 300 nm before and after each cycle of deformation.

Figure 1 shows grain reference orientation deviation (GROD) EBSD maps of a sample as-received (Fig. 1a) and after each cycle of dynamic deformation (Fig. 1b and 1c). The GROD EBSD map illustrates local strain accumulation within a grain. The GROD map shows a deviation angle between any pixel in the grain and the average misorientation of the grain.

The as-received microstructure of the Mg sample is characterized by large grains (average size 150 μm) with numerous deformation twins ($86.3^\circ \langle 11\text{-}20 \rangle$). Some statistical recrystallized grains (average grain size of 10 μm) are also observed in 15% of the sample.

After the first cycle of dynamic deformation (Fig. 1b), a severe microstructure change is observed in the creation of ASB, which is characterized by a presence of dynamic recrystallized grains, which are observed in 35% (average grain size of 1.8 μm) of the sample. After the 2nd cycle of dynamic deformation, the crack formation is observed, with very fine grain structure around fissure (Fig. 1c). No strain accumulation around the crack and in ASB is observed from GROD maps. The grains are fully dynamic recrystallized.

It is well known that the EBSD lateral resolution for magnesium is about 600 nm (measured at an accelerating voltage of 15 keV [9]). To measure the grain size of magnesium in ASB around the crack, a thin lamella (electron-transparent sample) was prepared for transmission Kikuchi diffraction (TKD) analyses. The thin sample was prepared by standard in situ lift-out in a FIB system, and cleaned and thinned to a desired thickness using a concentrated (as small as 1 μm) argon ion beam [NanoMill[®] TEM specimen preparation system, Fischione Instruments]. TKD measurements were performed with an on-axis detector [Optimus, Bruker Nano Analytics] fitted on a FIB system, operated at 30 kV. Figure 2 represent GROD TKD maps acquired with a 20 nm step size, collected from an area close to the tip of

the crack. The average grain size measured from TKD analyses is 800 nm. No magnesium deformation twins or accumulation of dislocations (resulting in local misorientation accumulation) is observed.

A mechanism of cracking is proposed for pure magnesium, taking into account ASB formation and dynamic recrystallization. Under dynamic high strain loading conditions, the geometrically necessary dislocation (GND) density increases within the grains. To accommodate the strain, the grains tend to rotate and GND increase in the proximity of grain boundaries. With continuous deformation, the incoming dislocation density exceeds a grain boundary's absorption capacity and a new dynamic recrystallized grain nucleates. The presents of new dynamic recrystallized grains in ASB, results in material softening. The new grains deform consequently, with the strain leading to crack formation.

In our presentation, we will further investigate that hypothesis and present results from numerous microscopy and microanalysis investigations.

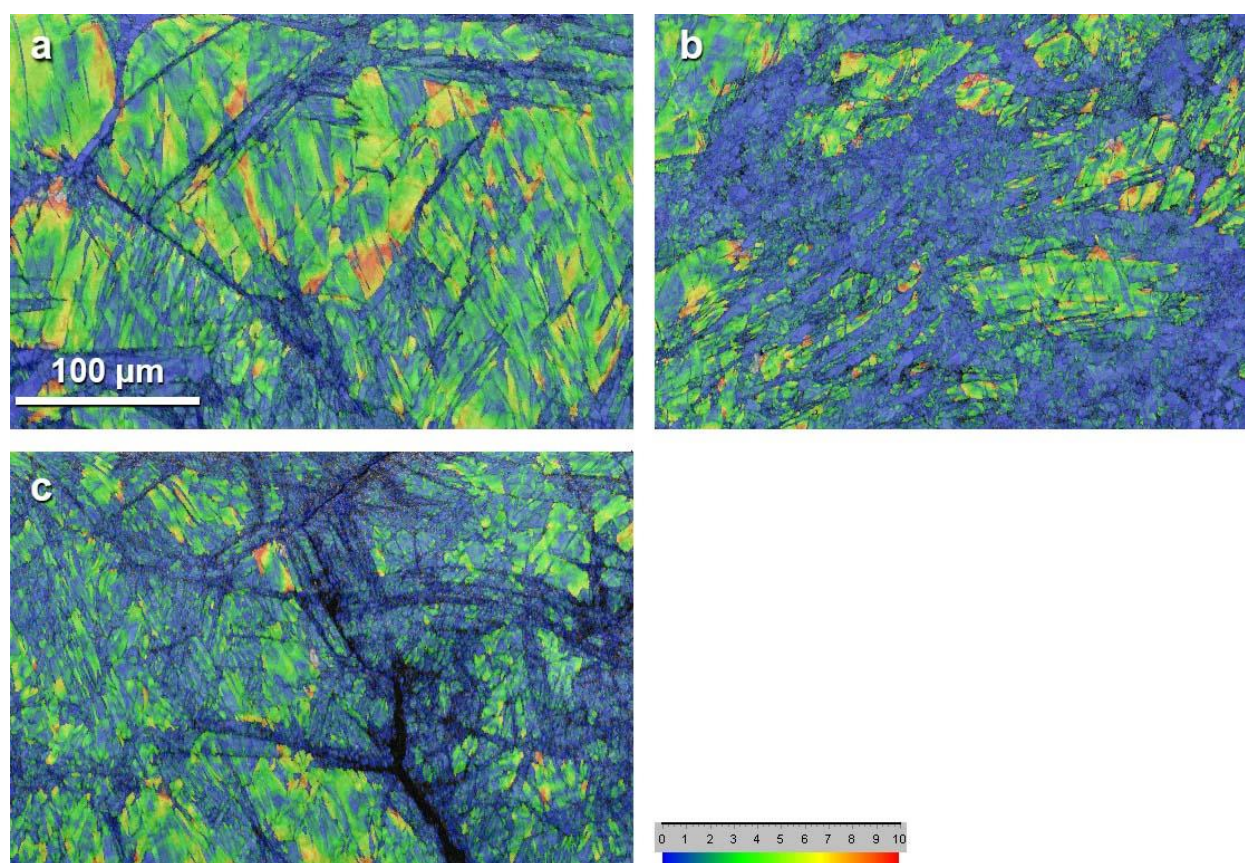


Figure 1. GROD EBSD maps of sample: (a) structure of sample as-received; (b) after first dynamic deformation cycle; and (c) after second dynamic deformation. Data collected at 15 kV acceleration voltage and 300 nm step size.

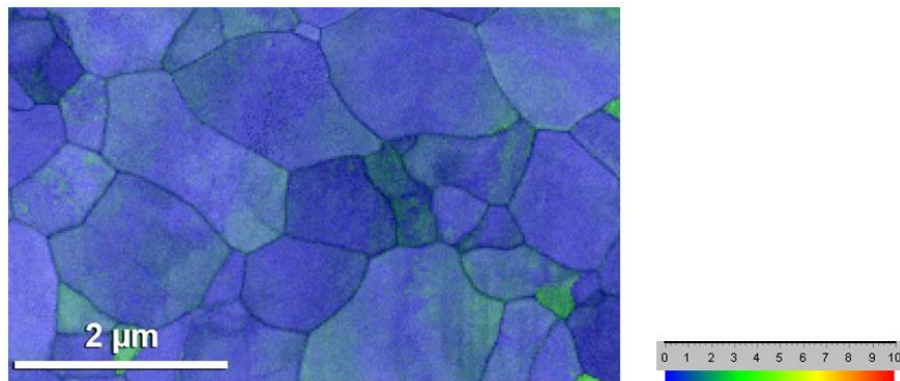


Figure 2. GROD TKD maps collected from an electron transparent sample, in an area close to the tip of the crack, following the second deformation cycle. Data collected at 30 kV acceleration voltage and 20 nm step size.

Reference

- [1] P Landau, S Osovski, A Venkert, V Gärtnerová, D Rittel, *Scientific Reports*, **6**(1) (2016). doi:10.1038/srep37226
- [2] X Zhu, Q Fan, D Wang, H Gong, Y Gao, F Qian, G Sha, *Scripta Materialia* **206** (2022), p. 114229. doi:10.1016/j.scriptamat.2021.114229
- [3] C Lieou, H Mourad, C Bronkhorst, *International Journal of Plasticity*, **119** (2019), p. 171-187. doi:10.1016/j.ijplas.2019.03.005
- [4] J Rodríguez-Martínez, G Vadillo, D Rittel, R Zaera, J Fernández-Sáez, *Mechanics of Materials*, **81** (2015), p. 41-55. doi:10.1016/j.mechmat.2014.10.001
- [5] D Rittel, P Landau, A Venkert, *Physical Review Letters*, **101**(16) (2008), p. 165501 doi:10.1103/physrevlett.101.165501
- [6] S Boakye-Yiadom, N Bassim, *Materials Science and Engineering: A* **711**(2018), p. 182-194. doi:10.1016/j.msea.2017.11.027
- [7] F Tetteh, S Duntu, S Boakye-Yiadom, *Microscopy and Microanalysis* **26**(S2) (2020), p. 1078-1080. doi:10.1017/s1431927620016888
- [8] Y Nie, B Claus, J Gao, X Zhai, N Kedir, J Chu, ... W Chen, *Experimental Mechanics* **60**(2) (2019), p. 153-163. doi:10.1007/s11340-019-00544-w
- [9] A Tripathi, S Zaeferrer, *Ultramicroscopy* **207** (2019), p. 112828. doi:10.1016/j.ultramic.2019.112828